

Looking at fault reactivation matching structural geology and seismological data

Cristiano Collettini^{a,*}, Lauro Chiaraluce^b, Stefano Pucci^{a,b}, Massimiliano R. Barchi^a,
Massimo Cocco^b

^a*Geologia Strutturale e Geofisica, Università degli Studi di Perugia, Italy*

^b*Istituto Nazionale di Geofisica e Vulcanologia, Rome, Italy*

Received 5 May 2004; received in revised form 7 October 2004; accepted 27 October 2004

Available online 29 April 2005

Abstract

We investigate fault reactivation that occurred during the 1997 Colfiorito seismic sequence (central Italy), matching detailed structural geology, precise earthquake locations and mechanical models of fault interaction. The Colfiorito area, within the Northern Apennines, is characterised by a relatively recent inversion of the tectonic stress field from compression (late Miocene), to extension (late Pliocene–Quaternary). In September–October 1997 the area experienced a protracted seismic sequence consisting of six moderate magnitude earthquakes ($5 < M_w < 6$), that ruptured SW-dipping normal fault segments. The two main ruptures of the sequence show opposite directions of rupture propagation and are segmented by a strike-slip fault inherited from the compressional tectonic phase. Late in the sequence this strike-slip fault nucleated an $M_w = 4.3$ event and an associated aftershock sequence, which we present as an example of reversal of fault slip direction. Plotting the strike-slip events on a detailed geological map, the left-lateral strike-slip fault imaged by aftershock distribution and focal mechanisms, strictly corresponds to the mapped $N10^\circ$ right-lateral strike-slip structure inherited from the compressional tectonic phase. The two different data-sets for this strike-slip fault show the same geometry but opposite kinematics.

We analyse the coseismic elastic static stress changes due to the occurrence of the normal fault events in order to investigate the mechanical coupling and interaction between the NW–SE oriented normal fault system and the intervening $N10^\circ$ inherited fault. We show that the elastic stress perturbation increased on the shallow portion of the activated volume where the $N10^\circ$ structure is located, and promoted its reactivation with a strike-slip motion. The different amount of slip experienced along the two normal faults responsible for the greater mainshocks favoured the left-lateral strike-slip kinematics.

© 2005 Elsevier Ltd. All rights reserved.

Keywords: Reactivation; Earthquakes; Fault zone; Apennines

1. Introduction

The term ‘fault reactivation’ assumes a slightly different meaning for structural geologists and seismologists. Within a seismically active region most of the earthquakes occur as reactivation of pre-existing faults or fault patches because this is mechanically easier than forming a new fault (Scholz, 1998). In this view, fault reactivation, governed by Amonton’s law, occurs every time the fault generates an earthquake (e.g. Sibson, 1990). This mechanistic meaning

of fault reactivation is useless for field geologists since the resolution of geological criteria cannot discriminate the effects of a single movement within fault zones. Field criteria, in fact, can address fault reactivation when the fault experienced a period of quiescence: therefore, fault reactivation acquires a geological meaning when discrete displacement events are separated in time (intervals > 1 Ma: Holdsworth et al., 1997).

Here we present an approach for investigating fault reactivation processes that matches detailed structural geology and precise earthquake locations. We use the term fault reactivation for a fault, documented with both geological and seismological criteria, which has been active with opposite kinematics during two distinct tectonic regimes (time interval ~ 2 Ma). For understanding why fault reactivation occurred in a specific location and with

* Corresponding author. Tel.: +39 75 5852651; fax: +75 5852603
E-mail address: colle@unipg.it (C. Collettini).

specific kinematics, we use static stress transfer modelling and analysis of mainshocks slip distribution.

2. Study area

The Northern Apennines are characterised by the presence of a complex pattern of thrusts, strike-slip faults, folds and normal faults, reflecting the superposition of two main tectonic phases (e.g. Lavecchia et al., 1994; Barchi et al., 1998; Tavarnelli, 1999): an Upper Miocene–Lower Pliocene compressional phase, forming an E–NE verging fold and thrust belt and a superimposed Upper Pliocene–Quaternary extensional phase, forming extensional basins bounded by NW–SE-trending normal faults. This latter phase produced in Umbria a 150-km-long alignment of NW–SE-trending, SW-dipping active normal faults (Umbria Fault System, inset of Fig. 1a), where the strongest historical (intensity = XI) and instrumental ($5.0 < M < 6.0$) seismicity occurs (e.g. CPTI, 1999; Barchi et al., 2000, and references therein).

Within this active alignment, the geological structures of the Colfiorito area define a highly segmented crustal portion (Fig. 1a). The contractional structures, striking mainly N–S, consist of W-dipping thrusts and associated box-shaped, E-verging anticlines, separated by narrow and deep synclines (Barchi et al., 2001). Folds and thrusts are accomplished by $N20^\circ \pm 10^\circ$ and $N110^\circ \pm 10^\circ$ striking transpressive faults, with right- and left-lateral kinematics, respectively, which are commonly interpreted as transfer faults or oblique/lateral ramps (e.g. Lavecchia et al. (1988) but see also Cello et al. (1997)). Contractional structures are displaced by a system of NW–SE-trending, normal faults that show a clear topographic signature and bound several small intramountain basins (Fig. 1a).

In September–October 1997, the Colfiorito area experienced a protracted seismic sequence (Fig. 1a) consisting of eight significant major earthquakes (Chiaraluca et al., 2003): a foreshock ($M_w = 4.5$, event 1), six extensional mainshocks ($5.0 < M_w < 6.0$, events from 2 to 7) and a subsequent strike-slip event ($M_w = 4.3$, event 8) that occurred in between the two larger extensional mainshocks (events 2 and 3). The precise aftershock locations, obtained by applying a double-difference location algorithm (Waldhauser and Ellsworth, 2000) on the data set collected by a dense local network (see Chiaraluca et al., 2003), allowed the reconstruction of the geometry of the activated normal fault system. Normal fault length is on the order of 5–10 km and segmentation is mainly controlled by pre-existing thrusts and/or strike-slip faults (Chiaraluca et al., 2005 and Fig. 1). The stress field, obtained by inverting the six mainshock focal mechanisms, reveals a clear NE-trending extension and the majority of the aftershocks ($\sim 70\%$) are consistent with the mainshock stress field (Chiaraluca et al., 2003). The distribution of the seismicity related to the strike-slip sub-sequence highlights a $N10^\circ$, ~ 7 -km-long,

left-lateral strike-slip structure (Fig. 1b) that extends from ~ 0.5 to ~ 3 km in cross-section (Fig. 1c). In the following, we are going to match seismological and geological data to present this strike-slip sub-sequence as an example of fault reactivation.

3. Matching seismology with structural geology for defining fault reactivation

The strike-slip fault is located in between the two major fault segments of the system (events 2 and 3). The opposite direction of rupture propagation, SE and NW for events 2 and 3, respectively (Pino and Mazza, 1999), and their fault architecture (Figs. 1a and b and 2a) points to an important role played by the strike-slip fault as a barrier in rupture propagation (cf. Chiaraluca et al., 2005 for details). The alignment, formed by the aftershock locations associated with the strike-slip event, identifies the $N10^\circ$ -trending, left-lateral strike-slip nodal plane as the true ruptured plane (Fig. 1b). Plotting the strike-slip sequence on the geological map, the left-lateral strike-slip fault imaged by aftershock distribution strongly corresponds to a mapped right-lateral strike-slip fault inherited from the compressional phase (Figs. 1a and 2a). In cross-section, the strike-slip rupture nucleates at a depth of 1 km and the aftershock distribution highlights a vertical structure down to 3 km deep, which merges at the surface with the outcropping strike-slip fault (Fig. 1c).

In order to characterise the geometry and kinematics of the strike-slip fault in the field, we collected data at different structural stations (see location on Fig. 2a). The fault zone is represented by a series of sub-vertical, $N10^\circ \pm 10^\circ$ -trending fault planes and reaches a maximum width of 1.5 km. The fault zone is characterised kinematically by sub-vertical C surfaces bounding S foliated domains, indicating a right-lateral sense of shear (Fig. 2b) and sub-vertical synthetic and antithetic riedels, again consistent with right-lateral kinematics (Fig. 2c).

Field geology and seismology data allow the definition of a strike-slip fault zone characterised by the same geometry and slip direction (Fig. 3a and b) but opposite kinematics: right-lateral for the mapped fault and left-lateral for the activated fault (Fig. 3c and d). Our conclusion is that the right-lateral strike-slip fault mapped at the surface was reactivated with opposite kinematics during the 1997 sequence: the same transfer fault accommodated differential displacement produced by thrusts during the compressional phase and by normal faults during the subsequent extensions (Fig. 3c and d).

4. Reactivation promoted by fault interaction

Several studies have proposed the coexistence of different mechanisms for earthquake triggering in the

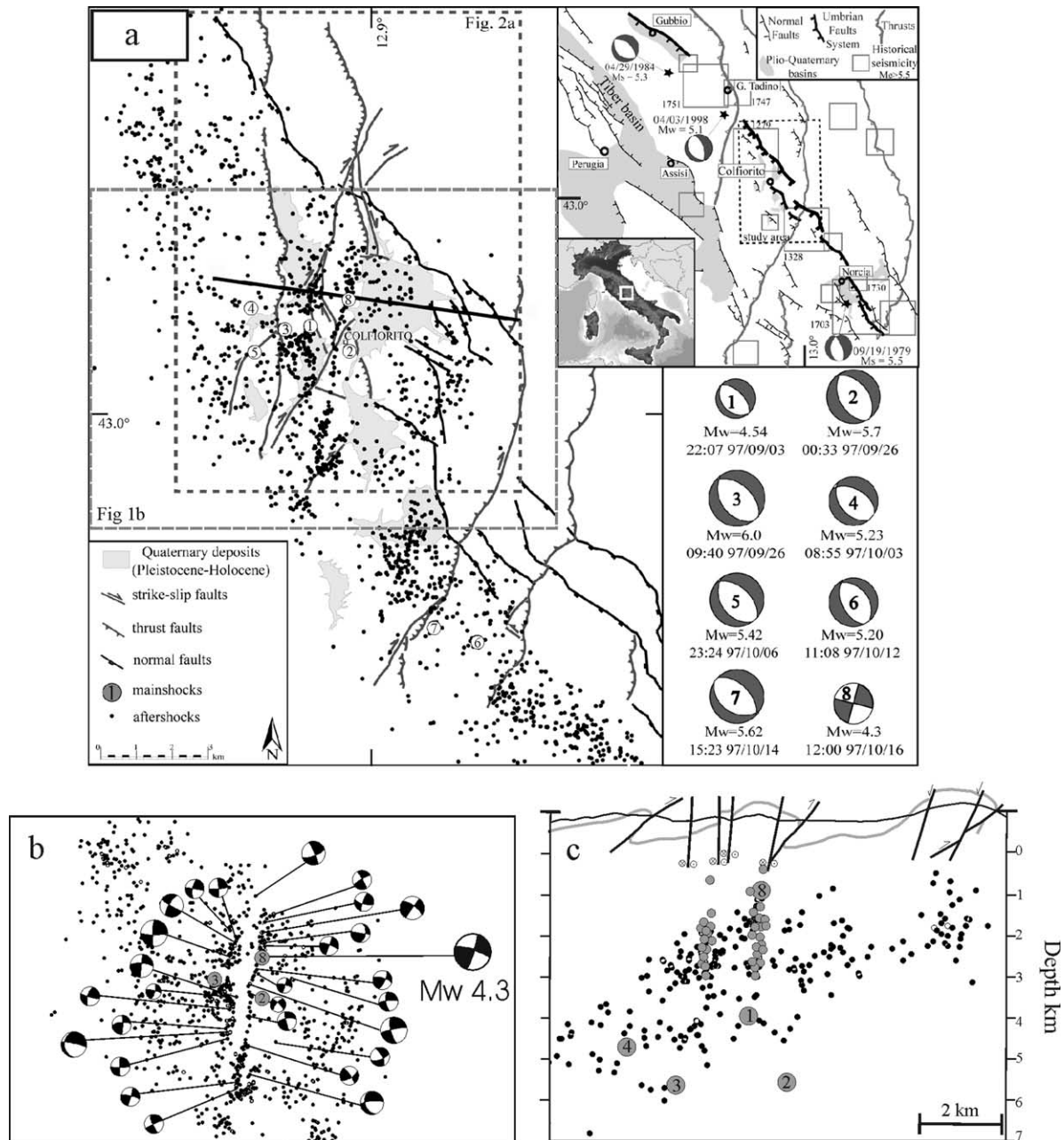


Fig. 1. (a) Structural map of the Colfiorito area derived from detailed field mapping, 1:10,000 scale (Barchi et al., 2001); note the right-lateral strike-slip fault located in the northern portion. Distribution of the Colfiorito 1997 seismic sequence (Chiaraluce et al., 2003) with the focal mechanisms of the mainshocks (Ekström et al., 1998). The inset shows the schematic distribution of the active normal faults in the Umbria region. (b) Aftershocks distribution and focal mechanisms of the left-lateral strike-slip sub-sequence (modified after Chiaraluce et al., 2003). (c) Cross-section (trace on (a)) integrating geological and seismological data; the grey line represents the attitude of the Marne a Fucoidi Fm. (Lower Cretaceous). The strike-slip aftershocks (small grey circles) highlight a vertical fault that merges at the surface with the mapped strike-slip structure. The earthquakes plotted in the cross-section are located within a band having a half-width of 2 km.

Colfiorito area, invoking either static stress changes (Cocco et al., 2000) or high fluid pressure (Miller et al., 2004). Here we are not going to analyse the physical processes controlling earthquake triggering, rather we use static stress transfer to investigate the orientation of the optimally oriented plane for Coulomb failure in the area where the mapped strike-slip fault crops out.

Static stress transfer in the neighbourhood of the causative fault (e.g. Stein, 1999; King and Cocco, 2001) can be evaluated by using the change in Coulomb Failure Stress (ΔCFS), which is defined as:

$$\Delta CFS = \Delta \tau + \mu(\Delta \sigma_n + \Delta P_f) \quad (1)$$

where $\Delta \tau$ is the shear stress change on the fault and $\Delta \sigma_n$ is

the normal stress change (positive for extension). ΔP_f is the change in pore pressure and μ is the friction coefficient. Failure is encouraged if ΔCFS is positive and discouraged if negative. We have computed elastic stress changes caused by an earthquake dislocation by solving the Volterra equation using the approach proposed by Okada (Okada, 1985, 1992) in an elastic homogeneous half space (see

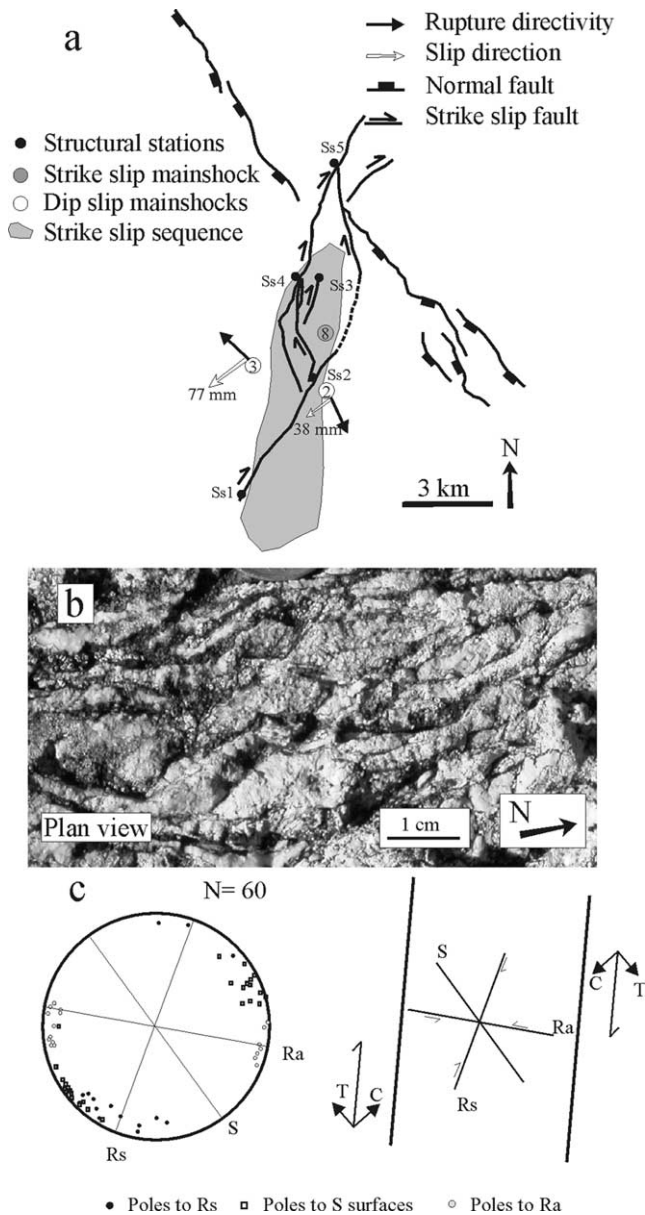


Fig. 2. (a) Schematic structural map showing the right-lateral strike-slip fault: the strike-slip structure separates the two normal faults that generated the strongest earthquakes (events 2 and 3). Vectors of rupture propagation after Pino and Mazza (1999). The direction of the slip vectors for the two mainshocks is derived from the focal mechanism solutions (Ekström et al., 1998), the amount of slip from InSAR interferometry and GPS measurements (Salvi et al., 2000). (b) Outcrop photograph showing the right-lateral strike-slip C/S fabric at Ss4. (c) Stereoplot (Schmidt equal area projection, lower hemisphere) of structural data collected at Ss4 (R_s, synthetic riedels; R_a, antithetic riedels; S, S-surfaces) and the inferred kinematics.

Nostro et al., 1997). For understanding the mechanical coupling between the strike-slip and the normal faults we calculated elastic stress changes caused by the preceding pure-extensional mainshocks and resolving the stress changes onto the positively discriminated N10° strike-slip structure, possessing a left lateral motion. The results of these calculations are shown in Fig. 4, which points out that the sequence of strike-slip earthquakes nucleates in an area of enhanced Coulomb stress both in map view (Fig. 4a) and cross-section (Fig. 4b); this area is elongated in the N10°-trending direction and corresponds to the mapped right-lateral strike slip structure. Thus our interpretation is that left-lateral strike-slip seismicity in this area is promoted by the elastic stress transferred by the normal faulting earthquakes.

The left-lateral strike-slip kinematics of the rupture is interpreted to be due to the different amount of slip that occurred on the two normal faults activated by the two

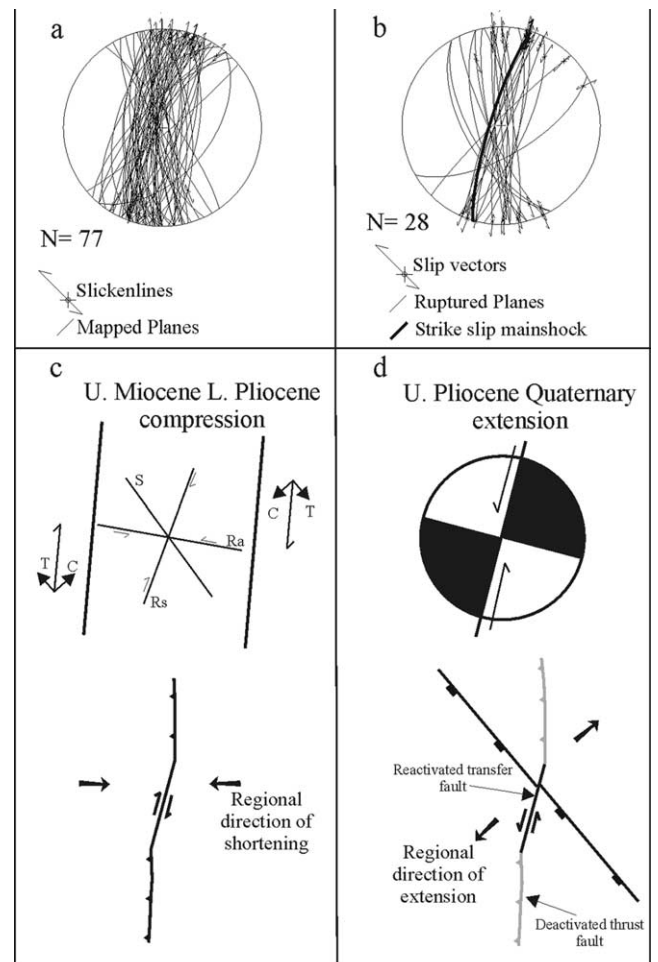


Fig. 3. Fault planes mapped at the surface (a) and ruptured fault planes derived from focal mechanisms (b) show the same ~N–S attitude and slip-direction but opposite kinematics. Stereoplots are represented as Schmidt equal area projection, lower hemisphere. Schematic evolution of the strike-slip fault: the fault was active as a right-lateral strike-slip structure during the Upper Miocene–Lower Pliocene compressional phase (c), then was reactivated as a left-lateral strike-slip fault during extension (d).

previous major earthquakes (Fig. 2a). Slip distribution modelling (Salvi et al., 2000) shows that the greater coseismic slip is concentrated in the hypocentral area, and the northern fault (event 3) experienced a greater slip (~ 77 cm) than the southern fault (event 2, ~ 38 cm). The different amount of slip occurring on these two adjacent faults results in a left-lateral strike-slip shear component along the intervening strike-slip zone. In addition, left-lateral kinematics is favoured by the orientation of the strike-slip fault with respect to the regional stress field depicted by the mainshocks (Fig. 3).

5. Conclusions

In a seismically active area characterised by recent reconfiguration of the stress regime, such as the Northern Apennines, inherited structures can play an important role

accommodating deformation in the ongoing stress field. A right-lateral strike-slip fault formed during the Upper Miocene–Lower Pliocene compressional phase acted as a barrier for rupture propagation during the 1997 Colfiorito extensional sequence, delimitating normal fault segments. At the end of the seismic crisis this strike-slip fault was activated by a left-lateral strike-slip sub-sequence. The reactivation of the strike-slip fault was promoted by the increase of stress generated by the previous normal faulting earthquakes. Fault reactivation was due to the different amount of slip experienced by the two major normal faults, inducing a left-lateral movement along the intervening fault zone. The re-utilisation of pre-existing planes, although with opposite kinematics, testifies to the importance of fault reactivation on seismic ruptures.

Acknowledgements

This research was supported by GNDT UR Perugia (grant awarded to Massimiliano Barchi, Perugia Research Unit Head) within the project: "Development and Comparison among Methodologies for the Evaluation of Seismic Hazard in Seismogenic Areas: Application to the Central and Southern Apennines", coordinated by M. Cocco. The authors thank N. De Paola for suggestions regarding the strike-slip fault and E. Tavarnelli, the Editor D. Ferrill and an anonymous reviewer for reviewing the manuscript.

References

- Barchi, M.R., Minelli, G., Piali, G., 1998. The crop 03 profile: a synthesis of results on deep structures of the Northern Apennines. *Memorie Società Geologica Italiana* 52, 383–400.
- Barchi, M.R., Galadini, F., Lavecchia, G., Messina, P., Michetti, A.M., Peruzza, L., Pizzi, A., Tondi, E., Vittori, E., 2000. Sintesi sulle conoscenze delle faglie attive in Italia Centrale. Gruppo Nazionale per la Difesa dei Terremoti, GNDT, 62pp.
- Barchi, M.R., Pucci, S., Collettini, C., Mirabella, F., Massoli, D., Guazzetti, F., Reichenbach, P., Cardinali, M., Vergoni, N., Troiani, E., Chiraz, P., Giombini, L., 2001. A geological map of the Colfiorito area. Federazione Italiana Scienze della Terra (FIST) annual meeting, 2001 Chieti.
- Cello, G., Mazzoli, S., Tondi, E., Turco, E., 1997. Active tectonics in the Central Apennines and possible implications for seismic hazard analysis in Peninsular Italy. *Tectonophysics* 272, 43–68.
- Chiaralucente, L., Ellsworth, W.L., Chiarabba, C., Cocco, M., 2003. Imaging the complexity of an active normal fault system: the 1997 Colfiorito (Central Italy) case study. *Journal of Geophysical Research* 108 (B6), 2294.
- Chiaralucente, L., Barchi, M.A., Collettini, C., Mirabella, F., Pucci, S., 2005. Connecting seismically active normal faults with Quaternary geological structures in a complex extensional environment: the Colfiorito 1997 case history (Northern Apennines, Italy). *Tectonics* 24, TC1002, doi:10.1029/2004TC001627.
- Cocco, M., Nostro, C., Ekstrom, G., 2000. Static stress changes and fault interaction during the 1997 Umbria–Marche earthquake sequence. *Journal of Seismology* 4, 501–516.
- CPTI, Gruppo di Lavoro, 1999. *Catálogo Parametrico dei Terremoti*

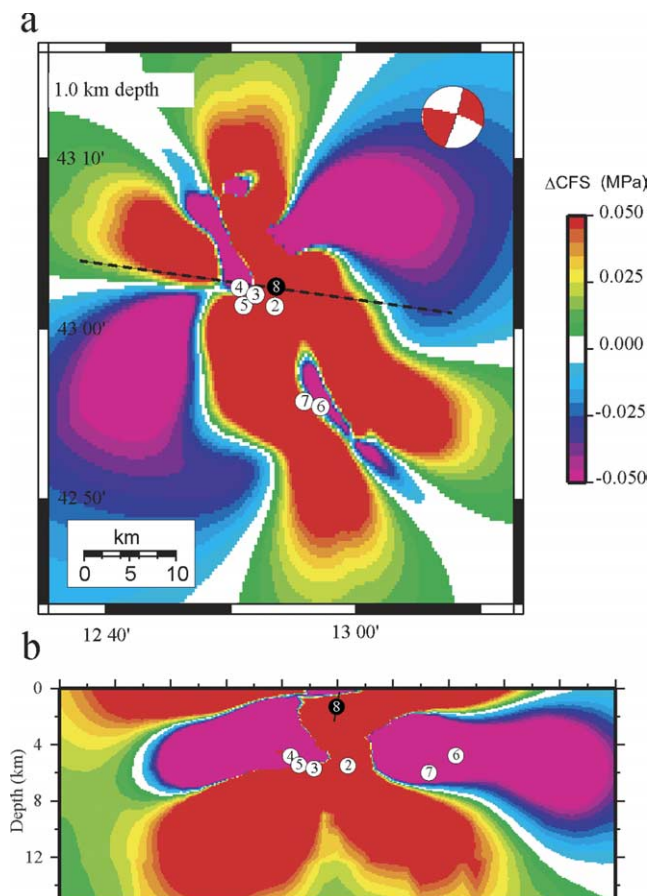


Fig. 4. Coulomb stress changes caused by the foreshock of September 3, 1997 and the six mainshocks that preceded the $M_w=4.3$ strike-slip event that has been located on the $N10^\circ$ -trending, inherited structure: (a) map view at 1 km depth (corresponding to the hypocentral depth of the $M_w=4.3$ strike-slip earthquake). (b) Cross-section: Coulomb stress modelling shows that normal faulting earthquakes increased the elastic stress along the $N10^\circ$ -trending structure, promoting seismicity with left-lateral strike slip mechanisms. These events activated a portion of the inherited structure that ruptured during the $M_w=4.3$ strike-slip sub-sequence.

- Italiani, Istituto Nazionale di Geofisica, Gruppo Nazionale per la Difesa dai Terremoti (GNDT), Storia Geofisica e Ambiente (SGA), Servizio Sismico Nazionale (SSN), Bologna, 92pp.
- Ekström, G., Morelli, A., Boschi, E., Dziewonski, A.M., 1998. Moment tensor analysis of the central Italy earthquake sequence of September–October 1997. *Geophysical Research Letters* 25, 1971–1974.
- Holdsworth, R.E., Butler, C.A., Roberts, A.M., 1997. The recognition of reactivation during continental deformation. *Journal of the Geological Society, London* 154, 73–78.
- King, G.C.P., Cocco, M., 2001. Fault interaction by elastic stress changes: new clues from earthquake sequences. *Advanced in Geophysics* 44, 1–38.
- Lavecchia, G., Brozzetti, F., Barchi, M., Menichetti, M., Keller, J.V.A., 1994. Seismotectonic zoning in east-central Italy deduced from analysis of the Neogene to present deformations and related stress fields. *Geological Society of America Bulletin* 106, 1107–1120.
- Lavecchia, G., Minelli, G., Piali, G., 1988. The Umbria–Marche arcuate fold belt (Italy). *Tectonophysics* 146, 125–137.
- Miller, S.A., Collettini, C., Chiaraluce, L., Cocco, M., Barchi, M., Boris, J.P.K., 2004. Aftershocks driver by a high-pressure CO₂ source at depth. *Nature* 427, 724–727.
- Nostro, C., Cocco, M., Belardinelli, M.E., 1997. Static stress changes in extensional regimes: an application to southern Apennines (Italy). *Bulletin Seismological Society of America* 87, 234–248.
- Okada, Y., 1985. Surface deformation due to shear and tensile faults in a half-space. *Bulletin Seismological Society of America* 75, 1135–1154.
- Okada, Y., 1992. Internal deformation due to shear and tensile faults in a half-space. *Bulletin Seismological Society of America* 82, 1018–1040.
- Pino, N.A., Mazza, S., 1999. Rupture directivity of the major shocks in the 1997 Umbria–Marche (Central Italy) sequence from regional broadband waveforms. *Geophysical Research Letters* 26, 2101–2104.
- Salvi, S., Stramondo, S., Cocco, M., Tesauro, M., Hunstad, I., Anzidei, M., Briole, P., Baldi, P., Sansosti, E., Fornaio, G., Lanari, R., Doumaz, F., Pesci, A., Galvani, A., 2000. Modeling coseismic displacements resulting from SAR interferometry and GPS measurements during the 1997 Umbria–Marche seismic sequence. *Journal of Seismology* 4, 479–499.
- Scholz, C.H., 1998. Earthquakes and friction laws. *Nature* 391, 37–42.
- Sibson, R.H., 1990. Rupture nucleation on unfavourably oriented faults. *Bulletin Seismological Society of America* 80, 1580–1604.
- Stein, R.S., 1999. The role of stress transfer in earthquake triggering. *Nature* 402, 605–609.
- Tavarnelli, E., 1999. Normal faults in thrust sheets: pre-orogenic extension, post-orogenic extension, or both? *Journal of Structural Geology* 21, 1011–1018.
- Waldhauser, F., Ellsworth, W.L., 2000. A double-difference earthquake location algorithm: method and application to the Northern Hayward Fault, California. *Bulletin Seismological Society of America* 90, 1353–1368.